HHS Public Access

Author manuscript

Cell Rep. Author manuscript; available in PMC 2021 January 26.

Published in final edited form as:

Cell Rep. 2021 January 12; 34(2): 108632. doi:10.1016/j.celrep.2020.108632.

Tet Proteins Regulate Neutrophil Granulation in Zebrafish through Demethylation of *socs3b* mRNA

Kelly M. Banks[1], **Yahui Lan**[1], **Todd Evans**[1,2,*]

[1]Department of Surgery, Weill Cornell Medicine, New York, NY 10065, USA

[2]Lead Contact

SUMMARY

Tet proteins (Tet1/2/3) convert 5-methylcytosine (5mC) to 5-hydroxy-methylcytosine (5hmC), initiating the process of active demethylation to regulate gene expression. Demethylation has been investigated primarily in the context of DNA, but recently Tet enzymes have also been shown to mediate demethylation of 5mC in RNA as an additional level of epitranscriptomic regulation. We analyzed compound *tet2/3* mutant zebrafish and discovered a role for Tet enzymes in the maturation of primitive and definitive neutrophils during granulation. Transcript profiling showed dysregulation of cytokine signaling in *tet* mutant neutrophils, including upregulation of *socs3b*. We show that Tet normally demethylates *socs3b* mRNA during granulation, thereby destabilizing the transcript, leading to its downregulation. Failure of this process leads to accumulation of *socs3b* mRNA and repression of cytokine signaling at this crucial step of neutrophil maturation. This study provides further evidence for Tets as epitranscriptomic regulatory enzymes and implicates Tet2/3 in regulation of neutrophil maturation.

Graphical Abstract

*Correspondence: tre2003@med.cornell.edu.

AUTHOR CONTRIBUTIONS

K.M.B. and T.E. designed the research plan, analyzed data, and wrote the manuscript. Y.L. provided essential advice and consultation and edited the manuscript. K.M.B. performed all the experiments.

SUPPLEMENTAL INFORMATION

Supplemental Information can be found online at https://doi.org/10.1016/j.celrep.2020.108632.

DECLARATION OF INTERESTS

The authors declare no competing interests.

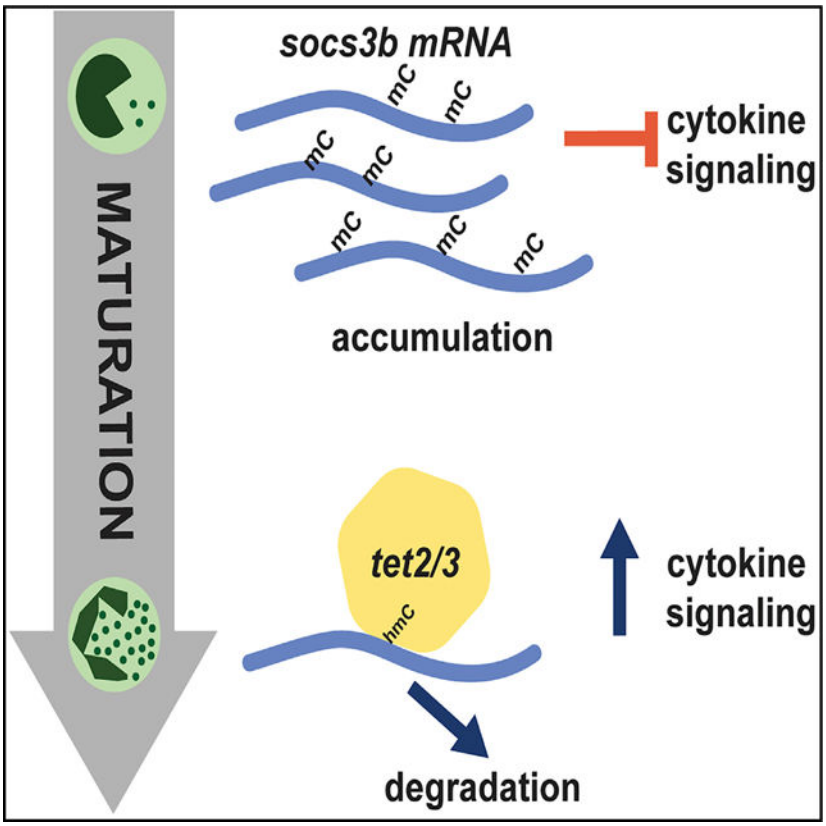

In Brief

Tet proteins are known for removing or blocking DNA methylation. Banks et al. show that zebrafish mutant for *tet2/3* have defects in maturation of primitive and definitive neutrophils. However, the phenotype is associated with hypermethylation of *socs3b* RNA, leading to enhanced *socs3b* RNA stability and a block in normal cytokine signaling.

INTRODUCTION

The ten-eleven translocation (Tet1/2/3) proteins are best known for their role as epigenomic regulators (controlling gene expression without altering DNA sequence) important for wide-ranging biological processes including hematopoiesis, somatic cell reprogramming, cancer pathogenesis, and early cell-fate determination (Pastor et al., 2013; Verma et al., 2018). Tet enzymes catalyze the conversion of 5-methylcytosine (5mC) to 5-hydroxy-methylcytosine (5hmC), which initiates the process of active demethylation, or may itself serve as a unique epigenomic signal (Pastor et al., 2013; Spruijt et al., 2013). Cytosine methylation in DNA plays a key role in transcriptional regulation of gene expression and, broadly speaking, is a repressive mark in gene regulatory elements (Pastor et al., 2013).

The emerging field of epitranscriptomics describes chemical RNA base modifications that serve as an additional layer of gene regulation (Saletore et al., 2012). The most abundant mark in mRNA is methyl-6-adenosine, involved in all aspects of RNA metabolism (Zhao et al., 2017). 5mC in RNA is the second most commonly observed base modification in mRNA

(Adams and Cory, 1975; Dubin and Taylor, 1975), generated primarily through the action of the RNA methyltransferase NSUN2 (Hussain et al., 2013; Squires et al., 2012; Yang et al., 2017). The discovery of 5hmC in RNA raised the possibility that, as for DNA, 5mC in RNA might be dynamically regulated, and indeed TET proteins were shown responsible for formation of 5hmC in RNA (Fu et al., 2014). Technical advances have allowed precise mapping of 5mC and 5hmC, which has shown a wide distribution for these modifications in mRNA (Delatte et al., 2016; Huber et al., 2015; Hussain et al., 2013). RNA bisulfite sequencing (RNA-BisSeq) was used to profile 5mC in mRNA from murine stem cells and brain, demonstrating an enrichment of the mark in nascent transcripts and translation start sites in both cell types and in 3′ UTRs in brain-derived mRNA, specifically (Amort and Lusser, 2017). Gene Ontology (GO) analysis revealed that uniquely methylated transcripts correlated with cell function. NSUN2 works together with ALYREF to promote export of methylated mRNA from the nucleus in HeLa cells (Yang et al., 2017). This report similarly demonstrated tissue-specific patterning of 5mC in mRNA through comparison of several murine tissues, again with uniquely methylated transcripts enriched in functionally relevant GO terms for each tissue type. 5mC was found mostly in coding regions, with a clear peak 100 bp downstream of the translation start site. Interestingly, the mean methylation level was only 20.5% at methylated sites and it did not occur exclusively in the CpG context (55% CG, 28% CHG, 17% CHH; H is A, C, or U). Finally, using a murine infection model, Tet2 was shown to demethylate the 3′ UTR of *Socs3* mRNA in mast cells, thereby destabilizing this transcript and leading to increased cytokine signaling and induction of emergency myelopoiesis (Shen et al., 2018). Following demethylation, a hairpin forms, allowing Adar1 binding and subsequent RNA degradation (Shen et al., 2018).

Knockout of murine *Tet1*, *Tet2*, and *Tet3* has demonstrated their importance in normal hematopoiesis across numerous lineages (Ichiyama et al., 2015; Langlois et al., 2014; Li et al., 2015; Lio et al., 2016; Montagner et al., 2016; Tsagaratou et al., 2017; Zhang et al., 2015). Generally, the observed phenotype is a block or delay in differentiation, sometimes with increased proliferative potential and/or dysregulation of key cytokines. Most of these studies identified interactions between TET proteins and key transcription factors (TFs) that facilitate targeting to specific regions of DNA. Tet function has been shown in mast cells, dendritic cells, T helper 1 (Th1) cells, Th17 cells, invariant natural killer T (iNKT) cells, B cells, and hematopoietic stem cells (HSCs), but the role of Tet proteins in neutrophils has not been specifically examined.

Neutrophils are a vital and abundant component of the innate immune system, comprising roughly 70% of circulating leukocytes (Dancey et al., 1976). Neutrophils respond rapidly to infection and are usually the first cells to arrive at the site of a wound or infection. Through degranulation, phagocytosis, and neutrophil extracellular trap (NET) formation, neutrophils destroy pathogens, and neutropenic patients are plagued by recurring bacterial and fungal infections (Skokowa et al., 2017). These strong histotoxic capabilities necessitate tight control, as hyperactive neutrophil function has been implicated in many pathologies, including various autoimmune (Kaplan and Radic, 2012), vascular (Döring et al., 2015), and renal diseases (Heinzelmann et al., 1999).

In zebrafish, hematopoiesis takes place in three waves: an initial primitive wave with spatially segregated myeloid (neutrophil, mast cell, and macrophage) and erythroid cells; a transient wave where erythromyeloid progenitors (EMPs) give rise to red blood cells, neutrophils, and mast cells; and, finally, the definitive wave, where HSCs are specified and give rise to all lineages including lymphoid cells from 5 days post fertilization (dpf) through adulthood (de Jong and Zon, 2005; Dobson et al., 2008). To explore functions for Tet proteins in neutrophils, we used a *tet2/3* double-mutant (*tet2/3*^{DM}) zebrafish model (Lan et al., 2019; Li et al., 2015). Previous work showed that Tet2 and Tet3 are the primary dioxygenases during zebrafish embryogenesis, with *tet2/3*^{DM} embryos essentially devoid of 5hmC (Li et al., 2015). These embryos fail to generate definitive HSCs, due to loss of key regulators of the endothelial-to-hematopoietic transition (EHT), including *runx1*, *gata2a*, and Notch signaling. In this study, we examined neutrophil development from the primitive and transient lineages in *tet2/3*^{DM} embryos, in addition to single-mutant and *tet2*$^{-/-}$ *tet3*$^{+/-}$ (*tet2/3*^{MH}) adults.

RESULTS

Myeloid Progenitors Are Specified in *tet* Mutant Embryos

To determine whether Tet proteins regulate neutrophil development, we performed whole-mount *in situ* hybridization (WISH) for myeloid markers during embryogenesis. Myeloid progenitors (MPs), the first committed myeloid cells of the primitive wave, arise primarily in the rostral blood island (RBI) located in the ventral cephalic mesoderm beginning at 16 h post fertilization (hpf). MPs are marked by transcripts for the TF *pu.1* and they persist until around 30 hpf (de Jong and Zon, 2005). All three *tet* isoforms are expressed in wild-type embryos at this early developmental stage and *tet2* and *tet3* are expressed in *pu.1+* progenitors (Figure S1). WISH for *pu.1* at 19.5 hpf and 25 hpf demonstrates that MPs emerge and proliferate in *tet2*$^{-/-}$, *tet3*$^{-/-}$, and *tet2/3*^{DM} embryos (Figures S1D–S1H). Although there is a trend toward fewer MPs in the *tet2/3*^{DM} embryos at 19.5 hpf, this difference is not statistically significant and nearly recovers by 25 hpf. We hypothesize that the slight reduction in number of MPs in *tet* mutants at 19 hpf is a delay in development of MPs rather than a true reduction or block in development of these cells. Whole-embryo qRT-PCR at 19.5 hpf demonstrates a reduction in transcripts encoding key myeloid TFs including *pu.1* and *cebpβ* in the *tet* mutant embryos compared with wild type (Figure S1I). *Pu.1* transcript levels are only reduced in the *tet2/3*^{DM} genotype, which could be partially explained by the reduction in MP number. However, *cebpβ* expression levels are sensitive to loss of even a single *tet* isoform. Taken together, it appears that Tet enzymes do not significantly impact the output of embryonic MPs yet play a role in fine-tuning the temporal expression of key TFs. Unlike for HSCs, *tet2* and *tet3* are not essential for specification of the primitive myeloid lineage. Of note, single-mutant *tet2*$^{-/-}$ and *tet3*$^{-/-}$ embryos show no morphological defects. Beginning at around 35 hpf, *tet2/3*^{DM} embryos have cerebral edema, smaller eyes, and a curved tail in comparison with wild type, as described in detail in our previous publication (Li et al., 2015).

Neutrophil Development Is Defective during Granule Formation in *tet3*$^{-/-}$ and *tet2/3*^{DM} Embryos

Primitive neutrophils differentiate from MPs beginning around 24 hpf, marked by expression of transcripts encoding the bactericidal enzyme myeloperoxidase (*mpx*), and they subsequently home to the ventral head and caudal hematopoietic tissue (CHT) regions (de Jong and Zon, 2005). During this time, transient lineage neutrophils also emerge in the CHT region from erythromyeloid progenitors (EMPs) at approximately 30 hpf. As primitive and transient neutrophils move through the proscribed stages of development (promyelocyte, myelocyte, metamyelocyte, band neutrophil, and finally segmented neutrophil), they undergo granulation (35–48 hpf) as well as morphological nuclear changes (Le Guyader et al., 2008). Interestingly, although there is no deficit in *mpx+* neutrophils at 2 dpf or 3 dpf (Figures 1A–1D, 1M, and 1N), many of these cells fail to properly granulate in *tet3*$^{-/-}$ and *tet2/3*^{DM} embryos, based on a reduction in the number of Sudan black (SB)-positive cells relative to *mpx*-positive cells at 3 dpf (Figures 1E–1H, 1M, and 1N). SB is a lipophilic dye that integrates into granule membranes and therefore marks only mature, granulated neutrophils. The population of *mpx*+ cells that are not SB+ represent immature neutrophils. At 2 dpf, these immature cells are present in all embryos and no difference is observed between genotypes (Figure 1M). At 3 dpf, we observe that only *tet3*$^{-/-}$ and *tet2/3*^{DM} have significant numbers of immature cells and significantly fewer SB+ mature cells than wild type and *tet2*$^{-/-}$ (Figure 1N). High-magnification views of SB+ cells show that the granulated cells of *tet3*$^{-/-}$ and *tet2/3*^{DM} embryos contain fewer granules than their wild-type and *tet2*$^{-/-}$ counterparts (Figures 1I–1L). Therefore, Tet proteins, in particular Tet3, are important for late differentiation and proper granulation of embryonic neutrophils.

In order to validate that this phenotype was caused by the loss of Tet3, we tested whether the granulation defect could be rescued by forced expression of RNA encoding wild-type or catalytically dead mutant human TET3 (hTET3). *TET3* is conserved between zebrafish and human, with 51.6% overall similarity and 100% alignment within key functional domains (Figure S2). We utilize *hTET3* because it provides validation that this is an evolutionarily conserved function of the enzyme. We injected 30 pg of *hTET3* mRNA into one-cell wild-type or *tet2/3*^{DM} embryos, and then quantified SB+ mature neutrophils by fixation, staining, and bright-field imaging of the same embryos at 3 dpf. Human wild-type *TET3* rescued the granulation of neutrophils in the CHT of *tet2/3*^{DM} embryos, but catalytically dead *hTET3* was not able to rescue granulation (Figure 2). Interestingly, when overexpressed in wild-type embryos, hTET3 caused an increased overall number of SB+ neutrophils (Figures 2A and 2C).

Neutrophil Phagocytosis Is Defective in *tet2/3*^{DM} Embryos

Given the developmental defect in *tet* mutant neutrophils, we investigated whether there were any corresponding functional defects. To this end, we utilized the pHrodo phagocytosis kit, in which phagocytosis is assayed using bioparticles conjugated to *E. coli* components and a pH-sensitive dye that fluoresces progressively more brightly in more acidic environments but is not detectable outside of the cell. The pHrodo bioparticles were injected into the circulation of 3-dpf *mpx:*GFP wild-type, *tet2*$^{-/-}$, *tet3*$^{-/-}$, and *tet2/3*^{DM} embryos, which were then imaged 2 h later using confocal microscopy (Figures 3A–3D). There were

significantly fewer beads phagocytosed in the *tet2/3*^{DM} neutrophils compared to wild type as measured by the area of the pHrodo fluorescent signal in pixels squared within *mpx*:GFP+ neutrophils of the CHT region (Figure 3E). Furthermore, the mean intensity of pHrodo fluorescence was significantly less in *tet2/3*^{DM} neutrophils compared to wild type, indicating that these phagosomes were also less acidic (Figure 3F). We performed the same experiment in *tet2*$^{-/-}$ *tet3*$^{+/-}$ neutrophils and also observed no defect compared to wild-type and *tet2*$^{-/-}$ neutrophils (Figures S3A–S3E). Interestingly, unlike the granulation defect, these phagocytosis defects were not observed in *tet3*$^{-/-}$ neutrophils, suggesting a more severe phenotype in the *tet2/3*^{DM} neutrophils or a separate mechanism regulating this process that can utilize either Tet2 or Tet3 interchangeably. We further probed the function of *tet2/3*^{DM} neutrophils in their ability to respond to injury using a tail injury assay. Briefly, we clipped the fin of 3-dpf *mpx*:GFP transgenic animals and then imaged 3 h later on a confocal microscope to quantify the number of GFP+ neutrophils recruited to the wound. We saw no defect in recruitment of neutrophils to the injury in *tet2/3*^{DM} embryos (Figures S3F–S3H). We hypothesize that response of neutrophils to the injury site develops relatively earlier in neutrophil differentiation such that these immature *tet2/3*^{DM} cells are still able to respond to injury through recruitment.

Aberrant Granule Formation in *tet2*$^{-/-}$*3*$^{+/-}$ Adult Neutrophils

We analyzed whether the findings in primitive and transient neutrophils also applied to adult, definitive-stage neutrophils. The *tet2/3*^{DM} genotype could not be used for an adult study as knockout of both *tet2* and *tet3* is embryonic lethal. Therefore, we utilized wild type, *tet2*$^{-/-}$, *tet3*$^{-/-}$, or *tet2*$^{-/-}$ (mutant; M) plus *tet3*$^{+/-}$ (heterozygous; H), hereafter referred to as *tet2/3*^{MH} for adult studies. The *tet2*$^{-/-}$, *tet3*$^{-/-}$, and *tet2/3*^{MH} fish appear normal with no gross anatomical defects. Kidneys were dissected from 1-year-old fish and flow cytometry was used with an established forward scatter and side scatter gating protocol to distinguish myeloid, hematopoietic progenitor, red blood cell (RBC), and lymphocyte fractions (Fan et al., 2014; Stachura et al., 2009). We observed a significant decrease in the percentage of cells in the myeloid fraction in *tet2*$^{-/-}$ and *tet2/3*^{MH} samples ($p = 0.003$, $p < 0.01$) and an increase in progenitors for the *tet2/3*^{MH} fish ($p = 0.0004$), suggesting a block in development of the *tet2/3*^{MH} myeloid cells (Figures 4A–4D and 4I). There was also a right shift in forward scatter area (FSC-A) values of the myeloid fraction in both *tet2*$^{-/-}$ and *tet2/3*^{MH} ($p = 0.0173$, $p = 0.0024$), demonstrating abnormal cell morphology (Figures 4A–4D, 4J, and 4K). Fluorescence-activated cell sorting (FACS)-purified myeloid cells were pelleted, embedded, and sectioned to perform electron microscopy. As in double-mutant embryos, we observed fewer granules per cell in the *tet2/3*^{MH} neutrophils, compared to wild-type or single-mutant neutrophils (Figures 4E–4H and 4L). Interestingly, there were additional abnormalities unique to the *tet2/3*^{MH} neutrophils, including increased incidence of autophagosomes and a wider nuclear envelope gap, perhaps indicative of defects in lipid processing within these cells (Figure 4H).

Transcript Profiling Shows Dysregulation of Cytokine Signaling in *tet* Mutant Neutrophils

We used a transgenic *mpx*:GFP zebrafish reporter line to isolate GFP+ neutrophils by FACS and performed bulk RNA sequencing (RNA-seq) (Yoo and Huttenlocher, 2011). Comparison of immature wild-type neutrophils (35 hpf) with 2-dpf neutrophils from wild-type, *tet2*$^{-/-}$,

tet3$^{-/-}$, and *tet2/3*^{DM} embryos showed distinct transcriptional patterns as assessed by principal component analysis (PCA; Figure 5A). Consistent with the granulation patterns described above, 2-dpf *tet3*$^{-/-}$ and *tet2/3*^{DM} samples clustered more closely and clearly separate from 2-dpf wild-type and *tet2*$^{-/-}$ samples. PC1 (Figure 5A) accounts for the most variation between 35-hpf and 48-hpf wild-type samples. The Database for Annotation, Visualization and Integrated Discovery Gene Ontology (DAVID GO) enrichment analysis for the top 100 differentially expressed genes within PC1 returned enrichment of terms including embryonic hematopoiesis ($p = 2.5 \times 10^{-8}$), myeloid cell differentiation ($p = 4.4 \times 10^{-4}$), and neutrophil differentiation ($p = 0.05$), indicating that PC1 identifies an axis of cell differentiation (Table S1). Interestingly, both *tet3*$^{-/-}$ and *tet2/3*^{DM} profiles were found midway between the 35-hpf wild-type and 2-dpf wild-type samples on PC1, indicating that *tet3*$^{-/-}$ and *tet2/3*^{DM} are less mature than stage-matched wild-type or *tet2*$^{-/-}$ neutrophils (Figure 5A). This is supported by the enrichment of several hematopoietic and myeloid differentiation GO terms representing gene sets with reduced expression levels in *tet2/3*^{DM} samples compared with wild-type samples (Figure 5B). The GO analysis of genes with reduced expression levels in *tet2/3*^{DM} samples also revealed downregulation of negative regulators of lymphocyte differentiation, which are normally upregulated as myeloid cells mature (Figure 5B). A few markers of neutrophil maturation downregulated in *tet2/3*^{DM} in the RNA-seq data were verified by qRT-PCR (Figure S4A). Also, both *tet3*$^{-/-}$ and *tet2/3*^{DM} neutrophils showed dysregulation of CCAAT-enhancer-binding protein (C/ebp) TFs and were enriched in a gene signature for C/ebpε-responsive genes (GSEA2186; Figures S4C–S4E) (Gombart et al., 2005). This further indicates that both *tet3*$^{-/-}$ and *tet2/3*^{DM} are not fully mature, as *C/EBPε* is active mostly during the myelocytic stage in human, when granules are still forming (Hsu et al., 2019). There is no direct *c/ebpε* ortholog in zebrafish, but the unique imbalance of *c/ebp* factors in *tet3*$^{-/-}$ and *tet2/3*^{DM} zebrafish neutrophils leads to the same transcriptional outcome of increased *C/ebpε* expression in immature human and mouse neutrophils. Compared to stage-matched wild-type cells, 4,573 genes are significantly dysregulated in *tet3*$^{-/-}$ neutrophils (2,268 upregulated and 2,305 downregulated) (Figure 5C) and 2,776 genes are significantly dysregulated (adjusted p value [p-adj] < 0.05) in *tet2/3*^{DM} neutrophils (1,297 upregulated and 1,479 downregulated) (Figure 5E). Strikingly, within the top 10 most significantly downregulated hallmark gene set enrichment analysis (GSEA) terms associated with *tet3*$^{-/-}$ and/or *tet2/3*^{DM} neutrophil samples are several cytokine signaling ontology terms: interleukin-6 (Il-6) Jak/Stat3 signaling, tumor necrosis factor α (Tnfα) signaling via nuclear factor kappa-light-chain-enhancer of activated B cells (NFKβ), interferon γ (Ifnγ) response, and Ifnα response (Figures 5D and 5F). Cytokine signaling, particularly through granulocyte colony-stimulating factor (G-CSF) and the Janus kinase/signal transducer and activator of transcription (Jak/STAT) pathway, is crucial in both normal and emergency granulopoiesis (Chakraborty and Tweardy, 1998).

Although there is a high degree of correlation between *tet3*$^{-/-}$ and *tet2/3*^{DM} samples both phenotypically and transcriptionally, they are distinct. This can be most readily observed using further PCA of PC2 (17% of variance) and PC3 (13% of variance) (Figure S4F). Hallmark GSEA comparing *tet3*$^{-/-}$ and *tet2/3*^{DM} indicates that *tet2/3*^{DM} samples have a more severe reduction of cytokine signaling response. Il-6 Jak/Stat3 signaling, inflammatory

response, allograft rejection, Ifnα response, Ifnγ response, and Tnfα signaling via NFKβ gene sets were all downregulated in *tet2/3*^{DM} (Figure S4G). Finally, we observed increased expression of cytokines in *tet3*$^{-/-}$ compared to *tet2/3*^{DM} neutrophils (Figure S4H). We hypothesize that the *tet3*$^{-/-}$ phenotype is partially compensated through upregulation of cytokines to overcome inhibition of downstream cytokine signaling, leading to a less severe phenotype.

Socs3b Transcript Levels Are Enhanced and Its Mutation Efficiently Rescues the Granulation Defect in *tet2/3*^{DM} Embryos

With respect to individual genes, we observed striking deregulation of *socs3b*, a member of the suppression of cytokine signaling gene family (Figure 6A). SOCS proteins bind the Jak receptor to prevent Stat phosphorylation and downstream signaling via the Jak/Stat pathway (Trengove and Ward, 2013). The *socs3b* gene is expressed at the highest levels of all SOCS isoforms in 2-dpf neutrophils, and transcript levels are significantly enhanced in immature 35-hpf wild-type, 2-dpf *tet3*$^{-/-}$, and 2-dpf *tet2/3*^{DM} neutrophils (Figure 6A). Increased *socs3b* expression in *tet2/3*^{DM} neutrophils was verified by qRT-PCR (Figure S4B). Because *Socs3*, the murine ortholog of *socs3b*, was shown to be regulated by Tet enzymes in mast cells (Shen et al., 2018), we hypothesized that *tet2/3* also directly regulates *socs3b* mRNA to mediate maturation and granulation of neutrophils. This is supported by the fact that *socs3b* transcript levels normally decrease between 35 hpf and 48 hpf in wild-type embryos (Figure 6A), suggesting the importance of regulating this gene for granulation, which occurs within that time window. To investigate the relevance of enhanced *socs3b* expression for the granulation defect we observed in *tet2/3*^{DM} embryos, CRISPR/Cas9 was used to mutate *socs3b* and evaluate whether the phenotype was rescued. Several single guide RNAs (sgRNAs) were tested and one was chosen that very efficiently generated targeted mutations near the start of the coding sequence for the Soc3b SH2 domain (Figures 6B and 6C). *Tet2/3*^{DM} embryos injected with this *socs3b* sgRNA and Cas9 protein had significantly more SB+ cells than uninjected *tet2/3*^{DM} embryos (Figures 6D–6F), rescued to wild-type levels. We were also able to rescue the granulation defect in *tet2/3*^{DM} embryos through microinjection into one-cell-stage embryos of 100 pg *csf3a* mRNA, the zebrafish ortholog of *G-CSF* (Figures S5A–S5C). Because SOCS proteins are known to inhibit Jak/Stat signaling downstream of G-CSF, this further demonstrates the importance of that pathway in causing the granulation defect in *tet* mutant embryos.

Socs3b mRNA Is Stabilized through Hypermethylation in *tet2/3*^{DM} Embryos

Because the genome of *tet* mutant fish is hypermethylated (Li et al., 2015), we first analyzed DNA methylation at the *socs3b* locus via enhanced reduced representation bisulfite sequencing (eRRBS) in GFP+ progenitors sorted from 17-hpf *pu.1:GFP* larvae or GFP+ neutrophils derived from *mpx:gfp* larvae at 2 dpf. The DNA samples from wild-type progenitors, wild-type neutrophils, and *tet2/3*^{DM} neutrophils all showed an identical highly methylated peak within a CpG island in the 5′ UTR and gene body of *socs3b* (Figures S5D and S5E). The eRRBS data showed only one differentially methylated region (DMR) in the 400 kb surrounding the *socs3b* locus, which was 150 kb upstream and hypermethylated in *tet2/3*^{DM} neutrophils (Figure S5D). The DMR lies within the first intron of a neighboring gene, *cyth1b*, and is potentially involved in promoter regulation of that locus; however, no

change in expression was observed for *cyth1b* in the RNA-seq data (Figure S5F). Although the *socs3b* gene is not differentially methylated, we mapped nearly 25,000 DMRs in the mutant neutrophils, the vast majority of which are hyper-DMRs (Figure S5G).

Shen et al. (2018) showed that in murine mast cells, *Socs3* expression levels are regulated through RNA methylation in the 3′ UTR rather than by DNA methylation. We therefore analyzed the methylation status of *socs3b* mRNA from wild-type or *tet2/3*^{DM} mutant neutrophils. A chi-square test demonstrated a significant increase in methylation of RNA from mutant neutrophils throughout the entire *socs3b* transcript ($p = 1.426 \times 10^{-4}$) with a peak within the coding sequence (Figure 7A). Of the top differentially methylated bases, 50% were CpG sites, 25% were CTG sites, and 25% were CHH sites (H is A, U, or C); this relative sequence promiscuity is consistent with earlier studies in RNA methylation (Yang et al., 2017). To determine the function of cytosine methylation in the *socs3b* mRNA, we mutated four of the top differentially methylated cytosines (DMCs) and injected wild-type and DMC mutant mRNA into wild-type embryos to monitor their relative stability over time. For this purpose, C-to-T transitions were edited at wobble positions in the coding DNA for cytosines showing 20% or more methylation change in *tet2/3*^{DM} neutrophils. These clustered within a small region of the mRNA, mutating only those bases that would not impact the amino acid coding sequence (Figure 7A, triangles). qRT-PCR using primers specific to injected mRNA demonstrated a faster rate of decay for the DMC mutant *socs3b* transcript. Transcript levels of injected *socs3b* transcripts were similar at 1 dpf, but by 2 dpf there were significantly lower levels in the DMC mutant condition ($p = 0.03$, n = 6 groups of 10 embryos/condition) (Figure 7B). This is reflected in the half-life of each mRNA from 1 dpf to 2 dpf, which was 0.175 for wild-type mRNA and 0.961 for DMC mutant mRNA. When the same experiment was carried out in *tet2/3*^{DM} embryos, no difference was observed between wild-type and DMC mutant mRNA stability (Figure S6A). In the *tet2/3*^{DM} embryos, the mRNA half-lives were 2.85 and 2.07 between 1.5 and 2 dpf, respectively. This further demonstrates that the difference in RNA stability is mediated through RNA demethylation, as there is no difference in stability when Tet protein function is abrogated.

Finally, we examined the *socs3b* RNA structure as predicted by minimum free energy (MFE) using the ViennaRNA package (Gruber et al., 2008). Interestingly, several DMCs were clustered within a single structural arm of the RNA highlighted in the inset of Figure 7C, indicated by triangles (red triangles represent bases mutated in generating the DMC mutant *socs3b* mRNA and black triangles represent DMCs that were not edited). The structure of this arm could potentially be perturbed by hypermethylation, possibly leading to destabilization by altering the RNA-binding protein (RBP) profile. The majority (7/9) of the DMCs are conserved across zebrafish, human, and mouse and the entirety of that RNA arm is well conserved by sequence (Data S1). We also investigated whether the RBP profile of the RNA arm is conserved using the RBPmap tool to search for motifs from the human/murine library in all species (Paz et al., 2014). We found that zebrafish had by far the most RBP motifs within this region, but there are several shared potential RBPs among all three species, many of which are involved in splicing (Figure S6B).

DISCUSSION

Tet enzymes have established roles in hematopoiesis across several lineages (Ichiyama et al., 2015; Langlois et al., 2014; Li et al., 2015; Lio et al., 2016; Montagner et al., 2016; Tsagaratou et al., 2017; Zhang et al., 2015), yet their role in neutrophil development or disease has not previously been evaluated. We found a defect in the maturation of neutrophils in *tet3*$^{-/-}$ and *tet2/3*^{DM} embryos and in *tet2/3*^{MH} adults such that these cells were blocked for maturation early in the granulation process. Tet3 appears to play a more important role in embryonic granulopoiesis whereas Tet2 is more important in definitive granulopoiesis. In both embryonic and adult cells, there is at least some compensation between the two Tet isoforms. This is perhaps because Tet2 requires additional proteins to allow binding to DNA/RNA, as it lacks the CXXC domain found in Tet1 and Tet3. In the adult cells, binding partners for Tet2 may allow it to function better in the adult context compared to primitive cells. Consistent with reports of developmental dysregulation in murine *Tet* knockout models for lymphoid and mast cells (Ichiyama et al., 2015; Montagner et al., 2016; Tsagaratou et al., 2017), we found that Tets regulate the maturation of neutrophils through control of cytokine signaling.

Tets are known primarily for regulating DNA demethylation. Previous studies to map DNA methylation changes over the course of granulopoiesis in mouse models (Bock et al., 2012; Deaton et al., 2011; Hogart et al., 2012) and sorted human primary cells (Chatterjee et al., 2015; Grassi et al., 2018; Rönnerblad et al., 2014) led to discordant results. The use of different methylation mapping formats may explain the different results and conclusions reported in those studies.

A recent report showed that in murine mast cells, TET2 regulates cytokine signaling not through DNA demethylation but through demethylation of the 3′ UTR of *Socs3* RNA (Shen et al., 2018), prompting us to evaluate the methylation status of the *socs3b* transcript in neutrophils. We observed a significant increase in methylation of the *socs3b* transcript in *tet2/3*^{DM} neutrophils compared with wild-type cells. However, in contrast to what was found in murine mast cells, most of the methylated cytosines were observed within the zebrafish *socs3b* gene body (coding sequence), with only one differentially methylated base in the 3′ UTR. Also, only half of the modified bases were in the CpG context, consistent with an earlier report characterizing 5mC in mRNA (Yang et al., 2017). In wild-type neutrophils, we observed downregulation of *socs3b* between 35 and 48 hpf, at precisely the time when neutrophils undergo granulation. Furthermore, we demonstrated the importance of reducing *socs3b* expression levels for neutrophil maturation as mutation of the gene in *tet2/3*^{DM} embryos rescued the granulation defect. By mutating the most highly methylated cytosine bases at wobble positions in *socs3b* mRNA, we were able to demonstrate that mutant (less methylated) *socs3b* transcripts are less stable when injected into wild-type embryos compared to the wild-type RNA.

We can now consider a dual-regulatory concept for Tet enzymes acting quickly to regulate transitory changes in gene expression through mRNA modification, as well as targeting DNA on an epigenomic timescale to commit cell-fate decisions and cell maturation and impart epigenomic memory. This could occur independently or simultaneously, perhaps

even through targeting the same nucleic acid sequence in mRNA or DNA. This could be particularly relevant in the context of neutrophil development and function because, in addition to epigenomic-based lineage control, epitranscriptomic regulation in these relatively short lived cells may underlie rapid activation and maturation to respond to infection.

A recent report characterized RNA methylation in very early zebrafish development (0–6 hpf), revealing its role in regulating the maternal-to-zygotic transition through stabilization of transcripts. At 6 hpf, the number of 5mC sites was dramatically reduced (2,902 sites) compared to 0 hpf (6,500 sites) (Yang et al., 2019). We find a similar mechanism of post-transcriptional regulation modulating RNA stability in our work, although it would appear additional methyl groups are deposited on the mRNA later in development. Because *socs3b* expression comes on and peaks at 1.5 dpf in neutrophils, we speculate that these m5C sites are being added sometime between 1 dpf and 1.5 dpf through the action of Nsun2, the ortholog of the primary RNA methyltransferase. Furthermore, our RNA-seq data from sorted neutrophils show that *nsun2* is the highest expressed of the NSUN gene family at both 35 hpf and 2 dpf (data not shown).

Double mutation of *tet2* and *tet3* likely causes developmental and functional defects through aberrant DNA methylation that may also impact these cells. In fact, RRBS revealed 21,338 hyper-DMRs and 2,554 hypo-DMRs at the DNA level comparing *tet2/3*^{DM} to wild-type 2-dpf neutrophils. However, the phenotype of neutrophil immaturity and reduced granule formation is most strongly impacted by demethylation of *socs3b* RNA rather than DNA demethylation of *socs3b* or its upstream activators. The Socs proteins are a part of a negative feedback loop regulated by cytokine signaling through the JAK/STAT pathway, so that it becomes difficult to parse out cause and effect of *socs3b* transcript-level upregulation. In examining differential expression of JAK/STAT family members and cytokines within the neutrophils using our RNA-seq data, we observe a few genes that are dysregulated above 2-fold with a p-adj < 0.05 (Figure S6C). Of these four factors, only *il1b* shows hyper-DMRs within 200 kb of the gene body, indicating that this gene may be directly controlled by Tet-mediated demethylation (Figure S6D). Although those genes that are downregulated are interesting in that they may be downstream of JAK/STAT inhibition by Socs3b (*jak3*, *il-10*, *csf1a*, and *il1b*), they cannot explain *socs3b* upregulation. Two of the differentially expressed factors are upregulated, namely *il-15l* and *csf3b* (one of two G-CSF orthologs in zebrafish). *Csf3b* has no DMRs within 200 kb of its gene body and therefore is unlikely regulated through DNA methylation. *Il-15l* has several DMRs within 200 kb that may impact its expression (Figure S6E), but this effect is likely minimal given its low expression level in comparison with other cytokines within these cells (Figure S6C). Therefore, *socs3b* RNA demethylation is likely the primary driver of this phenotype. Interestingly, both *csf3b* and *il-15l* are also increased in 35-hpf wild-type neutrophils compared to 2-dpf wild-type neutrophils and are likely more indicative of immaturity in the *tet2/3*^{DM} cells rather than pathologic (Figure S6C).

Limitations of Study

Although *socs3b* RNA is hypermethylated in Tet-deficient neutrophils, rescue of the maturation phenotype by injection of TET3 RNA does not target specifically neutrophils.

Therefore, it is possible that ectopic TET3 could impact methylation of *socs3b* RNA indirectly, even by changes in DNA methylation of other genes. A cell-autonomous function for Tet proteins in neutrophils could be more rigorously tested using a lineage-directed transgene, such as *mpx:TET3*, crossed onto the double-mutant background. This strategy was suggested in a reviewer's comments received May 5, 2020. Unfortunately, non-COVID research at our institution was closed down starting in mid-March. To make this transgenic strain and cross it onto the $tet23^{DM}$ background would take at least 1 year, which was prohibitive, especially because we were not allowed to breed animals during the pandemic shutdown. As we restart normal research operations, this strategy will be pursued. Also, we recognize that mutation of *tet2/3* likely also causes defects through DNA methylation and do not wish to imply that DNA methylation has no impact within these cells. Indeed, we present RRBS data to globally describe the presence of DMRs within the mutant cells. Rather, we restrict our conclusion to the phenotype of neutrophil immaturity and reduced granule formation that is most strongly impacted by demethylation of *socs3b* RNA rather than demethylation of *socs3b* DNA or its upstream activators. The focus on *socs3b* was justified because it was one of the most highly increased gene products in mutant neutrophils, and bioinformatic analyses failed to identify any alternative pathways implicated in neutrophil maturation. Finally, we feel there is an advantage in using the human *TET3* ortholog for rescue because it provides validation that this is an evolutionarily conserved function of the enzyme. However, future experiments can compare all three zebrafish orthologs to explore specificity of action.

STAR★METHODS

RESOURCE AVAILABILITY

Lead contact—Further information and requests for reagents should be directed to and will be fulfilled by the Lead Contact, Todd Evans (tre2003@med.cornell.edu).

Materials availability—All unique/stable reagents generated in this study are available from the Lead Contact with a completed Materials Transfer Agreement.

Data and code availability—RNA-sequencing and bisulfite sequencing data are available at the GEO data depository under accession number GSE162435.

EXPERIMENTAL MODEL AND SUBJECT DETAILS

Zebrafish were used with approval by the Weill Cornell Medicine (WCM) institutional animal care and use committee. We used 0–4 days post fertilization larval zebrafish for this study, bred on AB/TUB background. Zebrafish were raised under standard conditions at 28C and morphologically staged. No statistical methods were used to predetermine sample size, and animal selection was not randomized or blinded. Mutant fish lines utilized in this study include $tet2^{mk17/mk17}$ ($tet2^{-/-}$), $tet3^{mk18/mk18}$ ($tet3^{-/-}$) and $tet2^{mk17/mk17}$ $tet3^{mk18/+}$ ($tet2/3^{MH}$) (Li et al., 2015). Animals were genotyped as described (Li et al., 2015). The transgenic reporter line $mpx:GFP^{uwm1}$ was used for imaging and sorting larval GFP+ neutrophils (Yoo and Huttenlocher, 2011). The transgenic reporter line *pu.1*:GFP^{zdf11} was used for sorting GFP+ myeloid progenitors (Hsu et al., 2004). Embryos selected for

experiments were typically less than 4 dpf, a stage at which sex cannot be determined and is unlikely to influence the biological processes under study. For experiments using kidney marrow from adult fish, both male and female animals were included in the analysis, and results were not affected by sex.

METHOD DETAILS

Whole-mount *in situ* hybridization (WISH) and Sudan Black staining—Zebrafish embryos at defined stages were fixed in 4% paraformaldehyde. Whole-mount RNA *in situ* hybridization (WISH) was performed using standard methods and probe generation (Jowett, 1999). Probes were previously described: *pu.1* (Lieschke et al., 2002) and *mpx* (Thisse et al., 2001). Sudan Black staining for granules was performed as described previously using the KOH/H_2O_2 clearing protocol (Le Guyader et al., 2008).

pHrodo whole mount phagocytosis assay—3 dpf *mpx*:GFP transgenic zebrafish embryos were injected with 1 nL of 1 mg/ml pHRODO *E. coli* Red particles (Invitrogen). Systemic delivery was achieved by microinjection into the duct of Cuvier by two 0.5 nL injections at 12 psi. Embryos were then incubated in the dark for 2 hr before imaging in low melt agarose using a confocal microscope (Zeiss LSM800). Analysis was performed using MATLAB to filter for Red pHRODO beads within GFP+ neutrophils only and then using global thresholding to measure area and mean intensity of the pHRODO beads (Mathworks).

Fin clip neutrophil recruitment assay—3 dpf *mpx*:GFP transgenic zebrafish embryos were anesthetized in tricaine before completely transecting the tail fin tip with a clean razor blade. Embryos were then incubated in E3 for 3 h before imaging in low melt agarose using a confocal microscope (Zeiss LSM800). Analysis was performed by first creating a maximum intensity projection in ImageJ and manually quantifying GFP+ neutrophils recruited to the wound site.

RNA isolation and quantitative RT-PCR—Total RNA from whole embryos or sorted neutrophils was isolated with the RNeasy Mini kit (QIAGEN) or RNeasy Micro kit (QIAGEN). As *tet2/3*^{DM} embryos are not readily distinguished by morphology until 35 h post-fertilization (hpf), 19.5 hpf embryos were individually fin-clipped and genotyped for *tet2* and *tet3* allele status. During processing embryos were kept in RNA isolation buffer at −80C and pooled by genotype prior to extraction. At least 5 embryos or 5,000 neutrophils were used for each biological replicate. RNA was reverse transcribed with the Superscript III First-Strand Synthesis System (Invitrogen). The RT-qPCR analysis was performed on a LightCycler 480 II (Roche) using LightCycler 480 Sybr Green master mix (Roche). Primer sequences are provided in Table S2. Relative gene expression levels were determined as previously described using *eif1a* (*eef1a1l1*) as a reference gene (McCurley and Callard, 2008).

Flow cytometry of whole kidney marrow—Kidneys were dissected from 1 year old fish and prepared for flow as described previously (Fan et al., 2014; Gerlach et al., 2011). Samples were analyzed or sorted based on FSC and SSC using either an Attune NXT

(Thermo Fisher) or AriaII (BD Biosciences) machine (Fan et al., 2014). Data were analyzed in FlowJo software (Treestar).

Electron microscopy—Myeloid cells were isolated by FACS as described above. 500,000 cells were pelleted in EM fixation solution and submitted to the WCM Imaging Core Facility for processing and imaging. Five to ten representative cells were imaged and analyzed per genotype.

RNA sequencing—For RNA sequencing, total RNA from 2 dpf wild-type, *tet2*$^{-/-}$, *tet3*$^{-/-}$, and *tet2/3*^{DM} sorted neutrophils and 35 hpf wild-type sorted neutrophils were isolated as described above. 2 ng total RNA was submitted to the WCM Genomics Resources Core Facility for library preparation with the TruSeq RNA Library Prep Kit v2 (Illumina) and paired-end sequencing using the HiSeq4000 platform (Illumina). Reads were aligned to the GRCz10 reference genome using TOPHAT. Differential gene expression was performed using DeSeq2. Orthology to human genes were performed as described (Anelli et al., 2017). GSEA was carried out using a pre-ranked list of the significantly dysregulated genes ranked by log2-fold change.

Reduced representation bisulfite sequencing—DNA from 17 hpf wild-type sorted *pu.1+* myeloid progenitors or 2 dpf wild-type and tet2/3^{DM} sorted MPX+ neutrophils was isolated using the Blood & Tissue Kits (QIAGEN). At least 20,000 cells were collected for each biological group. Genomic DNA was submitted to the WCM Epigenomics core for eRRBS, which supported alignment and methylation extraction for eRRBS data as described (Rampal et al., 2014).

Socs3b mRNA bisulfite sequencing—5 ng of total RNA was bisulfite converted using the EZ RNA Methylation Kit (Zymo Research) and then reverse transcribed with the Superscript III First-Strand Synthesis System (Invitrogen). The *socs3b* transcript was then PCR amplified in fragments and each of these were TOPO cloned. Primers were designed using the Zymo bisulfite primer seeker software and are provided in Table S2. Ten colonies were sequenced per segment and aligned to the bisulfite converted *socs3b* transcript sequence. All CpGs were scored for methylation status on the basis of C to T conversion, as well as any cytosines outside of a CpG context that were methylated >20% and recorded. Statistical analysis was performed using a chi-square test of total methylation status across the entire transcript.

CRISPR mutagenesis—The *Socs3b* gRNA sequence was selected using the Benchling gRNA design software and crRNA was purchased from IDT. The gRNA sequence is provided in Table S2. 1000 pg of duplexed gRNA made according to manufacturer specifications and 500 pg of rhCas9 protein were co-injected into 1-cell embryos. Editing was assessed using a T7 endonuclease assay (NEB labs) per manufacturer instructions in pooled groups of 10 embryos. PCR primers for the T7 assay are provided in Table S2.

WT and mutant socs3b RNA synthesis and microinjection—Zebrafish *csf3a* and *socs3b* were cloned from cDNA generated from 2 dpf wild-type neutrophils. The cDNA was cloned into the TOPO Blunt vector, and primers are provided in Table S2. The *socs3b* cDNA

including untranslated regions were then cloned into the pCS2+ expression vector. The mutant *socs3b* variant was generated by changing all wobble-position cytosines with a methylation status >20% in the *tet2/3*^{DM} samples by ordering 200–300 base pair segments with mutated cytosines in the pUC57-Kan backbone (Genewiz) and sub-cloning these into the pCS2+*socs3b* construct. Changed bases were at positions 586, 631, 706 and 1048 as indicated in the supplemental DNA files. Sequences of all clones were confirmed by conventional DNA sequencing. The FH-TET3-pEF wild-type and HxD mutant constructs were purchased (Addgene Plasmid # 49446, 127896) (Ko et al., 2010). Capped mRNA was synthesized from these expression vectors using the mMESSAGE mMACHINE kit (Invitrogen) with Sp6 polymerase and purified using the MEGAclear kit (Thermo Fisher). For each experimental condition, mRNA was injected into at least 100 embryos derived from wild-type or *tet2/3*^{MH} intercrosses.

Socs3b RNA stability RT-qPCR assays—Total RNA from *socs3b* injected whole embryos was isolated and reverse transcribed as described above. For experiments in wild-type, 1, 2, 3, and 4 dpf embryos were used whereas for *tet2/3*^{DM} embryo experiments, 1.5 dpf, 2 dpf and 3 dpf were used as mutants cannot be distinguished phenotypically until 1.5 dpf. RT-qPCR was performed using primers that overlapped the exogenous construct (Table S2) such that only injected RNA is detected and measured over time. *18 s* was utilized as a reference gene. The rate of decay was then calculated by dividing relative expression at t_2 by relative expression at t_1, taking the negative natural log of this ratio and dividing by time.

QUANTIFICATION AND STATISTICAL ANALYSIS

Statistical analysis was performed using Graphpad Prism 8.1.2 unless otherwise indicated. Data comparing two samples were analyzed using Student's t test. Data for greater than two samples were analyzed using analysis of variance followed by Tukey post hoc test. The significance is indicated as *p < 0.05, **p < 0.01, ***p < 0.001, ****p < 0.0001, n.s. indicates not significant.

Supplementary Material

Refer to Web version on PubMed Central for supplementary material.

ACKNOWLEDGMENTS

The authors thank members of the Evans laboratory for helpful discussions throughout the study. The authors acknowledge excellent technical assistance from the WCM Genomics, Epigenomics, Flow Cytometry, and Microscopy and Image Analysis core facilities. The study was supported by a grant from the Tri-Institutional Stem Cell Initiative, Starr Foundation (2014-010 to T.E.). K.M.B. is supported by the WCM Medical Scientist Training Program (T32GM-007739) from the National Institutes of Health and the New York State Department of Health (NYSTEM training grant C32558GG).

REFERENCES

Adams JM, and Cory S (1975). Modified nucleosides and bizarre 5′-termini in mouse myeloma mRNA. Nature 255, 28–33. [PubMed: 1128665]

Amort T, and Lusser A (2017). Detection of 5-methylcytosine in specific poly(A) RNAs by bisulfite sequencing. Methods Mol. Biol 1562, 107–121. [PubMed: 28349457]

Anelli V, Villefranc JA, Chhangawala S, Martinez-McFaline R, Riva E, Nguyen A, Verma A, Bareja R, Chen Z, Scognamiglio T, et al. (2017). Oncogenic BRAF disrupts thyroid morphogenesis and function via twist expression. eLife 6, e20728. [PubMed: 28350298]

Bock C, Beerman I, Lien WH, Smith ZD, Gu H, Boyle P, Gnirke A, Fuchs E, Rossi DJ, and Meissner A (2012). DNA methylation dynamics during *in vivo* differentiation of blood and skin stem cells. Mol. Cell 47, 633–647. [PubMed: 22841485]

Chakraborty A, and Tweardy DJ (1998). Stat3 and G-CSF-induced myeloid differentiation. Leuk. Lymphoma 30, 433–442. [PubMed: 9711905]

Chatterjee A, Stockwell PA, Rodger EJ, Duncan EJ, Parry MF, Weeks RJ, and Morison IM (2015). Genome-wide DNA methylation map of human neutrophils reveals widespread inter-individual epigenetic variation. Sci. Rep 5, 17328. [PubMed: 26612583]

Dancey JT, Deubelbeiss KA, Harker LA, and Finch CA (1976). Neutrophil kinetics in man. J. Clin. Invest 58, 705–715. [PubMed: 956397]

Deaton AM, Webb S, Kerr AR, Illingworth RS, Guy J, Andrews R, and Bird A (2011). Cell type-specific DNA methylation at intragenic CpG islands in the immune system. Genome Res. 21, 1074–1086. [PubMed: 21628449]

de Jong JL, and Zon LI (2005). Use of the zebrafish system to study primitive and definitive hematopoiesis. Annu. Rev. Genet 39, 481–501. [PubMed: 16285869]

Delatte B, Wang F, Ngoc LV, Collignon E, Bonvin E, Deplus R, Calonne E, Hassabi B, Putmans P, Awe S, et al. (2016). RNA biochemistry. Transcriptome-wide distribution and function of RNA hydroxymethylcytosine. Science 351, 282–285. [PubMed: 26816380]

Dobson JT, Seibert J, Teh EM, Da'as S, Fraser RB, Paw BH, Lin TJ, and Berman JN (2008). Carboxypeptidase A5 identifies a novel mast cell lineage in the zebrafish providing new insight into mast cell fate determination. Blood 112, 2969–2972. [PubMed: 18635811]

Döring Y, Drechsler M, Soehnlein O, and Weber C (2015). Neutrophils in atherosclerosis: from mice to man. Arterioscler. Thromb. Vasc. Biol 35, 288–295.

Dubin DT, and Taylor RH (1975). The methylation state of poly A-containing messenger RNA from cultured hamster cells. Nucleic Acids Res. 2, 1653–1668. [PubMed: 1187339]

Fan HB, Liu YJ, Wang L, Du TT, Dong M, Gao L, Meng ZZ, Jin Y, Chen Y, Deng M, et al. (2014). miR-142–3p acts as an essential modulator of neutrophil development in zebrafish. Blood 124, 1320–1330. [PubMed: 24990885]

Fu L, Guerrero CR, Zhong N, Amato NJ, Liu Y, Liu S, Cai Q, Ji D, Jin SG, Niedernhofer LJ, et al. (2014). Tet-mediated formation of 5-hydroxyme-thylcytosine in RNA. J. Am. Chem. Soc 136, 11582–11585. [PubMed: 25073028]

Gerlach GF, Schrader LN, and Wingert RA (2011). Dissection of the adult zebrafish kidney. J. Vis. Exp (54), 2839. [PubMed: 21897357]

Gombart AF, Krug U, O'Kelly J, An E, Vegesna V, and Koeffler HP (2005). Aberrant expression of neutrophil and macrophage-related genes in a murine model for human neutrophil-specific granule deficiency. J. Leukoc. Biol 78, 1153–1165. [PubMed: 16204633]

Grassi L, Pourfarzad F, Ullrich S, Merkel A, Were F, Carrillo-de-Santa-Pau E, Yi G, Hiemstra IH, Tool ATJ, Mul E, et al. (2018). Dynamics of transcription regulation in human bone marrow myeloid differentiation to mature blood neutrophils. Cell Rep. 24, 2784–2794. [PubMed: 30184510]

Gruber AR, Lorenz R, Bernhart SH, Neuböck R, and Hofacker IL (2008). The Vienna RNA websuite. Nucleic Acids Res. 36, W70–W74. [PubMed: 18424795]

Heinzelmann M, Mercer-Jones MA, and Passmore JC (1999). Neutrophils and renal failure. Am. J. Kidney Dis 34, 384–399. [PubMed: 10430993]

Hogart A, Lichtenberg J, Ajay SS, Anderson S, NIH Intramural Sequencing Center; Margulies EH, and Bodine DM. (2012). Genome-wide DNA methylation profiles in hematopoietic stem and progenitor cells reveal overrepresentation of ETS transcription factor binding sites. Genome Res. 22, 1407–1418. [PubMed: 22684279]

Hsu K, Traver D, Kutok JL, Hagen A, Liu TX, Paw BH, Rhodes J, Berman JN, Zon LI, Kanki JP, and Look AT (2004). The pu.1 promoter drives myeloid gene expression in zebrafish. Blood 104, 1291–1297. [PubMed: 14996705]

Hsu BE, Tabariès S, Johnson RM, Andrzejewski S, Senecal J, Lehuédé C, Annis MG, Ma EH, Völs S, Ramsay L, et al. (2019). Immature low-density neutrophils exhibit metabolic flexibility that facilitates breast cancer liver metastasis. Cell Rep. 27, 3902–3915.e6. [PubMed: 31242422]

Huber SM, van Delft P, Mendil L, Bachman M, Smollett K, Werner F, Miska EA, and Balasubramanian S (2015). Formation and abundance of 5-hydroxymethylcytosine in RNA. ChemBioChem 16, 752–755. [PubMed: 25676849]

Hussain S, Sajini AA, Blanco S, Dietmann S, Lombard P, Sugimoto Y, Paramor M, Gleeson JG, Odom DT, Ule J, and Frye M (2013). NSun2-mediated cytosine-5 methylation of vault noncoding RNA determines its processing into regulatory small RNAs. Cell Rep. 4, 255–261. [PubMed: 23871666]

Ichiyama K, Chen T, Wang X, Yan X, Kim BS, Tanaka S, Ndiaye-Lobry D, Deng Y, Zou Y, Zheng P, et al. (2015). The methylcytosine dioxygenase Tet2 promotes DNA demethylation and activation of cytokine gene expression in T cells. Immunity 42, 613–626. [PubMed: 25862091]

Jowett T (1999). Analysis of protein and gene expression. Methods Cell Biol. 59, 63–85. [PubMed: 9891356]

Kaplan MJ, and Radic M (2012). Neutrophil extracellular traps: double-edged swords of innate immunity. J. Immunol 189, 2689–2695. [PubMed: 22956760]

Ko M, Huang Y, Jankowska AM, Pape UJ, Tahiliani M, Bandukwala HS, An J, Lamperti ED, Koh KP, Ganetzky R, et al. (2010). Impaired hydroxylation of 5-methylcytosine in myeloid cancers with mutant TET2. Nature 468, 839–843. [PubMed: 21057493]

Lan Y, Pan H, Li C, Banks KM, Sam J, Ding B, Elemento O, Goll MG, and Evans T (2019). TETs regulate proepicardial cell migration through extracellular matrix organization during zebrafish cardiogenesis. Cell Rep. 26, 720–732.e4. [PubMed: 30650362]

Langlois T, da Costa Reis Monte-Mor B, Lenglet G, Droin N, Marty C, Le Couédic JP, Almire C, Auger N, Mercher T, Delhommeau F, et al. (2014). TET2 deficiency inhibits mesoderm and hematopoietic differentiation in human embryonic stem cells. Stem Cells 32, 2084–2097. [PubMed: 24723429]

Langmead B, and Salzberg SL (2012). Fast gapped-read alignment with Bowtie 2. Nat. Methods 9, 357–359. [PubMed: 22388286]

Le Guyader D, Redd MJ, Colucci-Guyon E, Murayama E, Kissa K, Briolat V, Mordelet E, Zapata A, Shinomiya H, and Herbomel P (2008). Origins and unconventional behavior of neutrophils in developing zebrafish. Blood 111, 132–141. [PubMed: 17875807]

Li C, Lan Y, Schwartz-Orbach L, Korol E, Tahiliani M, Evans T, and Goll MG (2015). Overlapping requirements for Tet2 and Tet3 in normal development and hematopoietic stem cell emergence. Cell Rep. 12, 1133–1143. [PubMed: 26257178]

Lieschke GJ, Oates AC, Paw BH, Thompson MA, Hall NE, Ward AC, Ho RK, Zon LI, and Layton JE (2002). Zebrafish SPI-1 (PU.1) marks a site of myeloid development independent of primitive erythropoiesis: implications for axial patterning. Dev. Biol 246, 274–295. [PubMed: 12051816]

Lio CW, Zhang J, González-Avalos E, Hogan PG, Chang X, and Rao A (2016). Tet2 and Tet3 cooperate with B-lineage transcription factors to regulate DNA modification and chromatin accessibility. eLife 5, e18290. [PubMed: 27869616]

McCurley AT, and Callard GV (2008). Characterization of housekeeping genes in zebrafish: male-female differences and effects of tissue type, developmental stage and chemical treatment. BMC Mol. Biol 9, 102. [PubMed: 19014500]

Montagner S, Leoni C, Emming S, Della Chiara G, Balestrieri C, Barozzi I, Piccolo V, Togher S, Ko M, Rao A, et al. (2016). TET2 regulates mast cell differentiation and proliferation through catalytic and non-catalytic activities. Cell Rep. 15, 1566–1579. [PubMed: 27160912]

Pastor WA, Aravind L, and Rao A (2013). TETonic shift: biological roles of TET proteins in DNA demethylation and transcription. Nat. Rev. Mol. Cell Biol 14, 341–356. [PubMed: 23698584]

Paz I, Kosti I, Ares M Jr., Cline M, and Mandel-Gutfreund Y (2014). RBPmap: a web server for mapping binding sites of RNA-binding proteins. Nucleic Acids Res. 42, W361–W367. [PubMed: 24829458]

Rampal R, Alkalin A, Madzo J, Vasanthakumar A, Pronier E, Patel J, Li Y, Ahn J, Abdel-Wahab O, Shih A, et al. (2014). DNA hydroxymethylation profiling reveals that WT1 mutations result in loss of TET2 function in acute myeloid leukemia. Cell Rep. 9, 1841–1855. [PubMed: 25482556]

Rönnerblad M, Andersson R, Olofsson T, Douagi I, Karimi M, Lehmann S, Hoof I, de Hoon M, Itoh M, Nagao-Sato S, et al.; FANTOM Consortium (2014). Analysis of the DNA methylome and transcriptome in granulopoiesis reveals timed changes and dynamic enhancer methylation. Blood 123, e79–e89. [PubMed: 24671952]

Saletore Y, Meyer K, Korlach J, Vilfan ID, Jaffrey S, and Mason CE (2012). The birth of the epitranscriptome: deciphering the function of RNA modifications. Genome Biol. 13, 175. [PubMed: 23113984]

Schneider CA, Rasband WS, and Eliceiri KW (2012). NIH Image to ImageJ: 25 years of image analysis. Nat. Methods 9, 671–675. [PubMed: 22930834]

Shen Q, Zhang Q, Shi Y, Shi Q, Jiang Y, Gu Y, Li Z, Li X, Zhao K, Wang C, et al. (2018). Tet2 promotes pathogen infection-induced myelopoiesis through mRNA oxidation. Nature 554, 123–127. [PubMed: 29364877]

Skokowa J, Dale DC, Touw IP, Zeidler C, and Welte K (2017). Severe congenital neutropenias. Nat. Rev. Dis. Primers 3, 17032. [PubMed: 28593997]

Spruijt CG, Gnerlich F, Smits AH, Pfaffeneder T, Jansen PW, Bauer C, Münzel M, Wagner M, Müller M, Khan F, et al. (2013). Dynamic readers for 5-(hydroxy)methylcytosine and its oxidized derivatives. Cell 152, 1146–1159. [PubMed: 23434322]

Squires JE, Patel HR, Nousch M, Sibbritt T, Humphreys DT, Parker BJ, Suter CM, and Preiss T (2012). Widespread occurrence of 5-methylcytosine in human coding and non-coding RNA. Nucleic Acids Res. 40, 5023–5033. [PubMed: 22344696]

Stachura DL, Reyes JR, Bartunek P, Paw BH, Zon LI, and Traver D (2009). Zebrafish kidney stromal cell lines support multilineage hematopoiesis. Blood 114, 279–289. [PubMed: 19433857]

Thisse B, Pflumio S, Fürthauer M, Loppin B, Heyer V, Degrave A, Woehl R, Lux A, Steffan T, Charbonnier XQ, and Thisse C (2001). Expression of the zebrafish genome during embryogenesis. ZFIN direct data submission. http://zfin.org.

Trengove MC, and Ward AC (2013). SOCS proteins in development and disease. Am. J. Clin. Exp. Immunol 2, 1–29. [PubMed: 23885323]

Tsagaratou A, González-Avalos E, Rautio S, Scott-Browne JP, Togher S, Pastor WA, Rothenberg EV, Chavez L, Lähdesmäki H, and Rao A (2017). TET proteins regulate the lineage specification and TCR-mediated expansion of iNKT cells. Nat. Immunol 18, 45–53. [PubMed: 27869820]

Verma N, Pan H, Doré LC, Shukla A, Li QV, Pelham-Webb B, Teijeiro V, González F, Krivtsov A, Chang CJ, et al. (2018). TET proteins safeguard bivalent promoters from *de novo* methylation in human embryonic stem cells. Nat. Genet 50, 83–95. [PubMed: 29203910]

Yang X, Yang Y, Sun BF, Chen YS, Xu JW, Lai WY, Li A, Wang X, Bhattarai DP, Xiao W, et al. (2017). 5-methylcytosine promotes mRNA export—NSUN2 as the methyltransferase and ALYREF as an m^5C reader. Cell Res. 27, 606–625. [PubMed: 28418038]

Yang Y, Wang L, Han X, Yang WL, Zhang M, Ma HL, Sun BF, Li A, Xia J, Chen J, et al. (2019). RNA 5-methylcytosine facilitates the maternal-to-zygotic transition by preventing maternal mRNA decay. Mol. Cell 75, 1188–1202.e11. [PubMed: 31399345]

Yoo SK, and Huttenlocher A (2011). Spatiotemporal photolabeling of neutrophil trafficking during inflammation in live zebrafish. J. Leukoc. Biol 89, 661–667. [PubMed: 21248150]

Zhang Q, Zhao K, Shen Q, Han Y, Gu Y, Li X, Zhao D, Liu Y, Wang C, Zhang X, et al. (2015). Tet2 is required to resolve inflammation by recruiting Hdac2 to specifically repress IL-6. Nature 525, 389–393. [PubMed: 26287468]

Zhao BS, Roundtree IA, and He C (2017). Post-transcriptional gene regulation by mRNA modifications. Nat. Rev. Mol. Cell Biol 18, 31–42. [PubMed: 27808276]

Highlights

- Zebrafish with compound *tet2/3* mutations show defects in neutrophil maturation
- Defects are associated with altered cytokine signaling and increased *socs3b* mRNA
- The *socs3b* mRNA rather than the gene itself is hypermethylated
- The data further support Tets as epitranscriptomic regulatory proteins

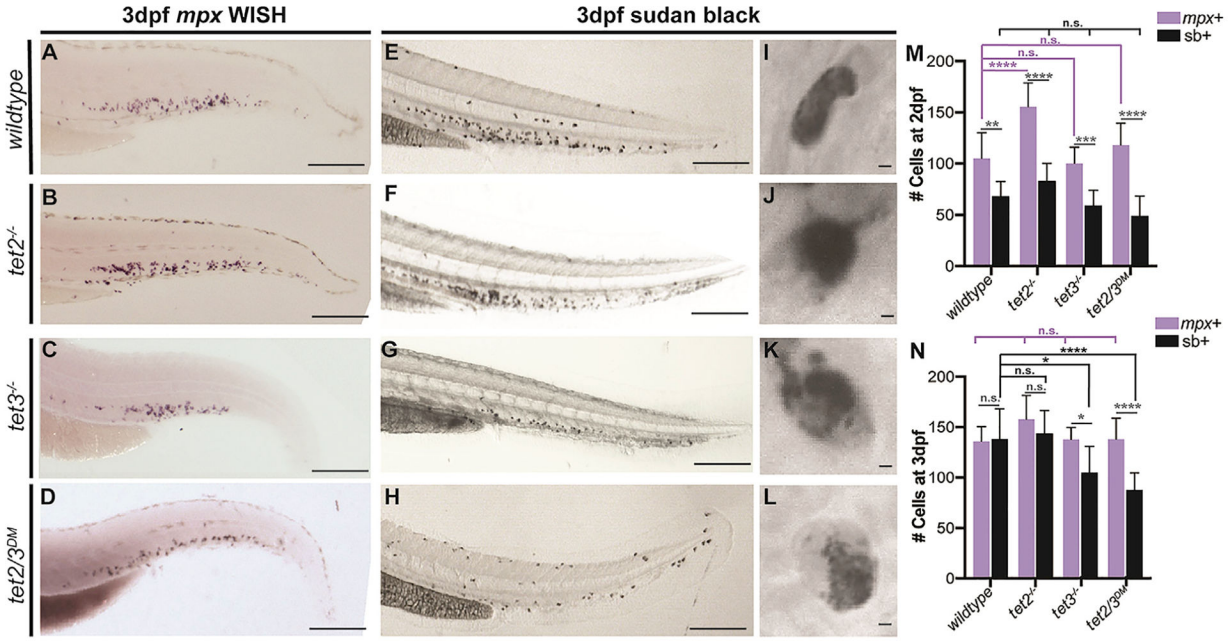

Figure 1. Granulation Is Defective in *tet3*$^{-/-}$ and *tet2/3*^{DM} Embryonic Neutrophils

Representative images of neutrophil staining in wild-type, *tet2*$^{-/-}$, *tet3*$^{-/-}$, and *tet2/3*^{DM} embryos at 3 dpf.

(A–D) Caudal hematopoietic tissue (CHT) region following WISH to analyze *mpx* transcripts.

(E–H) CHT region of embryos stained for Sudan black (SB). Scale bars in (A)–(H) represent 200 μm.

(I–L) High-resolution images of SB-stained neutrophils. Scale bars represent 2 μm.

(M and N) Quantification of total *mpx*+ (immature and mature neutrophils) and SB+ (mature neutrophils) cells in embryos at 2 dpf (M) and 3 dpf (N); n = 10/condition, *p < 0.05, ***p < 0.001, ****p < 0.0001 by 2-way ANOVA with Tukey post hoc test.

See also Figure S1.

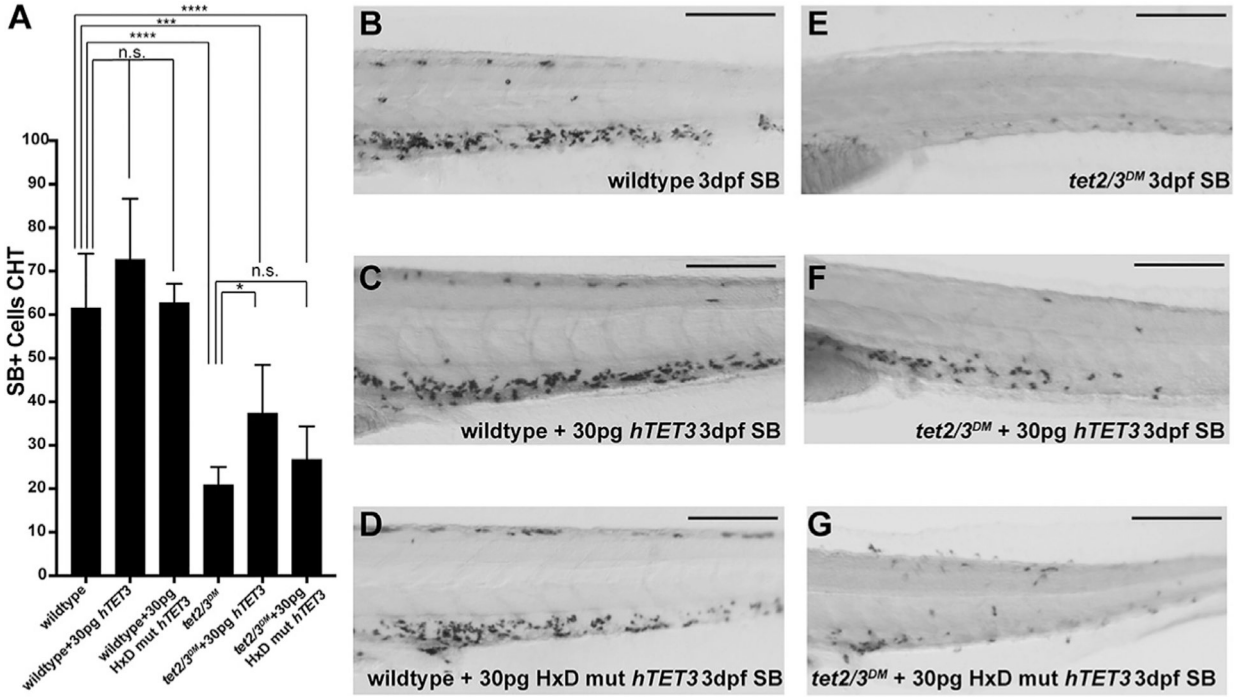

Figure 2. Human TET3 Overexpression Rescues the Granulation Defect in *tet2/3*^{DM} Embryos

(A) Quantification of SB+ cells in the CHT region for uninjected, 30 pg wild-type *hTET3* and 30 pg catalytically dead mutant (HxD) *hTET3*-injected wild-type and *tet2/3*^{DM} embryos at 3 dpf; n = 6/condition, *p < 0.05, ***p < 0.001, ****p < 0.0001 by 2-way ANOVA with Tukey post hoc test.

(B–G) Representative images of the CHT of SB-stained uninjected, wild-type *hTET3*-injected, or mutant *hTET3*-injected wild-type and *tet2/3*^{DM} embryos at 3 dpf. Scale bars represent 200 μm. See also Figure S2.

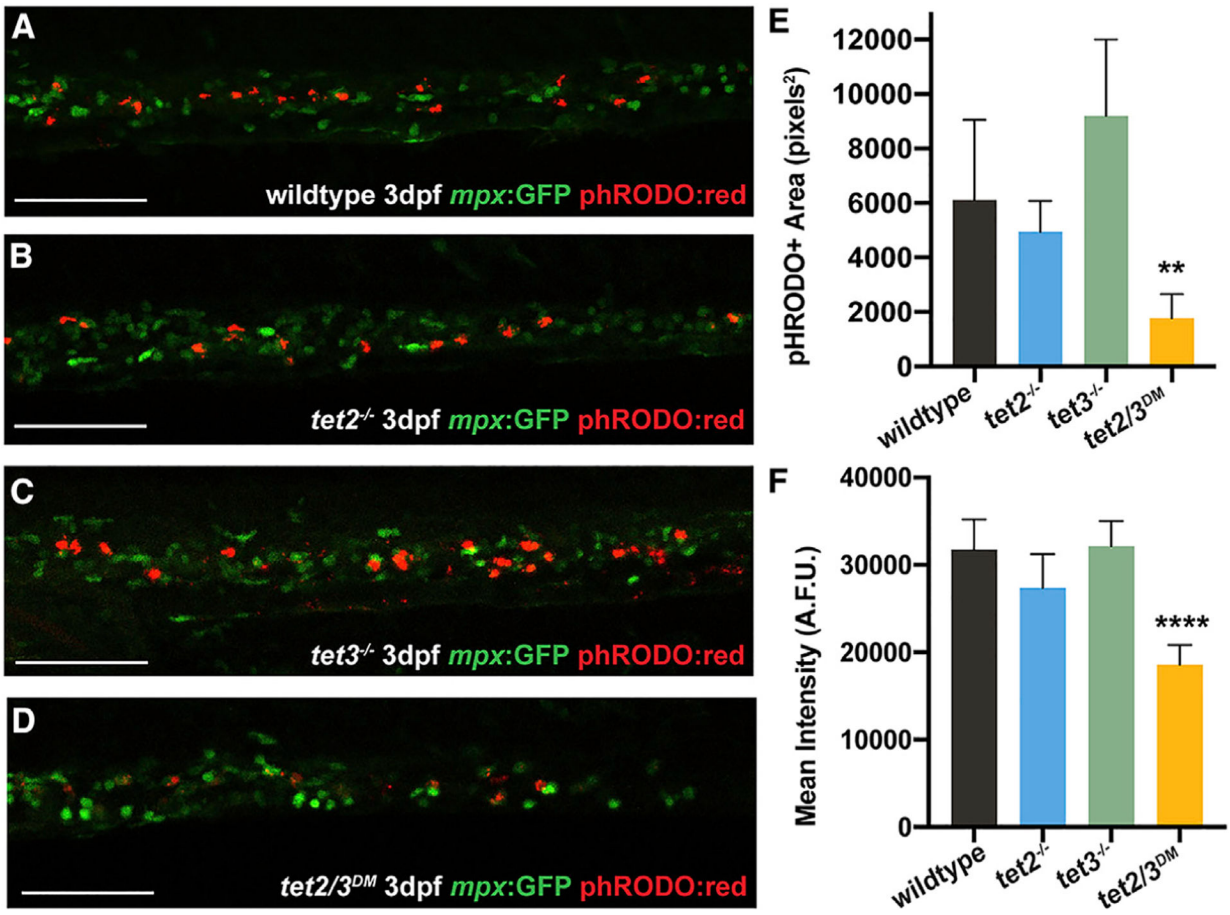

Figure 3. Phagocytosis Defect Is Unique to *tet2/3*^{DM} Embryonic Neutrophils

(A–D) Representative images of the CHT region in pHrodo-red-injected 3-dpf wild-type, *tet2*$^{-/-/}$, *tet3*$^{-/-}$, and *tet2/3*^{DM} *mpx*:GFP embryos. Scale bars represent 200 μm.

(E) Quantification of phagocytosed beads by fluorescent area within GFP+ neutrophils in pixels squared.

(F) Quantification of lysosome acidification by mean fluorescence intensity in arbitrary fluorescence units (A.F.U.).

n = 5–7 embryos/condition, **p < 0.01, ****p < 0.0001 by 2-way ANOVA with Tukey post hoc test of each condition compared to wild type. See also Figure S3.

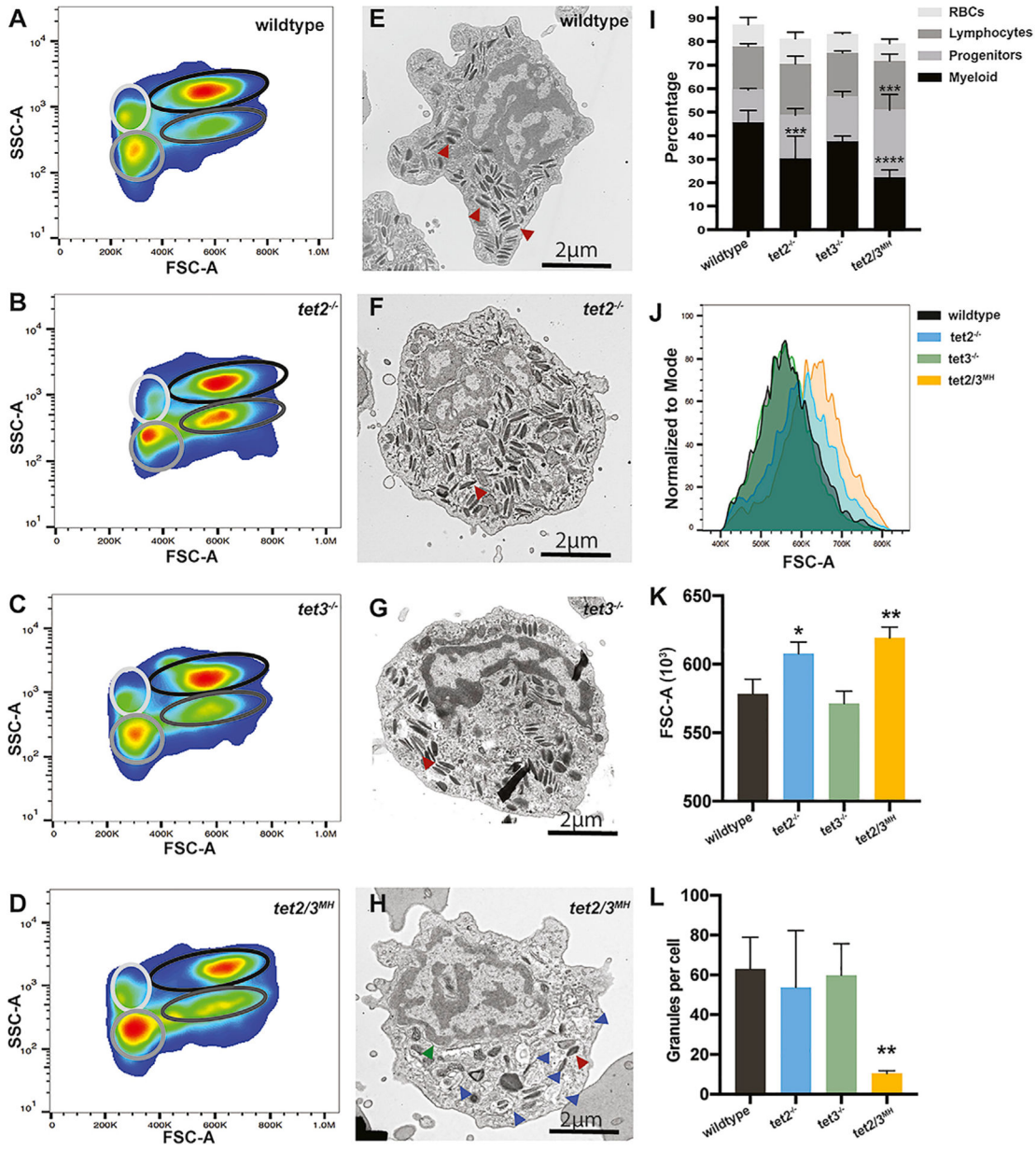

Figure 4. Granulation Defects Are Also Found in *tet2/3*^{MH} Adult Neutrophils

(A–D) Representative flow cytometry analysis of whole-kidney marrow (WKM) for 1-year-old wild-type, *tet2*$^{-/-}$, *tet3*$^{-/-}$, and *tet2/3*^{MH} zebrafish. Myeloid cells are delineated by the black circle, hematopoietic progenitors by a dark gray circle, lymphocytes by a medium gray circle, and red blood cells (RBCs) by a light gray circle.

(E–H) Representative electron microscopy images of wild-type, *tet2*$^{-/-}$, *tet3*$^{-/-}$, and *tet2/3*^{MH} neutrophils isolated by FACS from kidneys of 1-year-old adult zebrafish. Red arrowheads indicate representative granules, blue arrowheads indicate autophagosomes, and the green arrowhead indicates nuclear envelope separation.

(I) Quantification of the percentage of cells of each subtype: myeloid cells, progenitors, lymphocytes, and RBCs; n = 3/condition.

(J) Histogram comparing FSC-A for the myeloid gate in each genotype for a representative sample.
(K) Quantification of mean FSC-A for the myeloid gate in each genotype; n = 3/condition.
(L) Quantification of granules per cell in electron microscopy images; n = 4/condition.
*p < 0.05, **p < 0.01, ***p < 0.001, ****p < 0.0001 compared to wild type by one-way ANOVA with Tukey post hoc test.

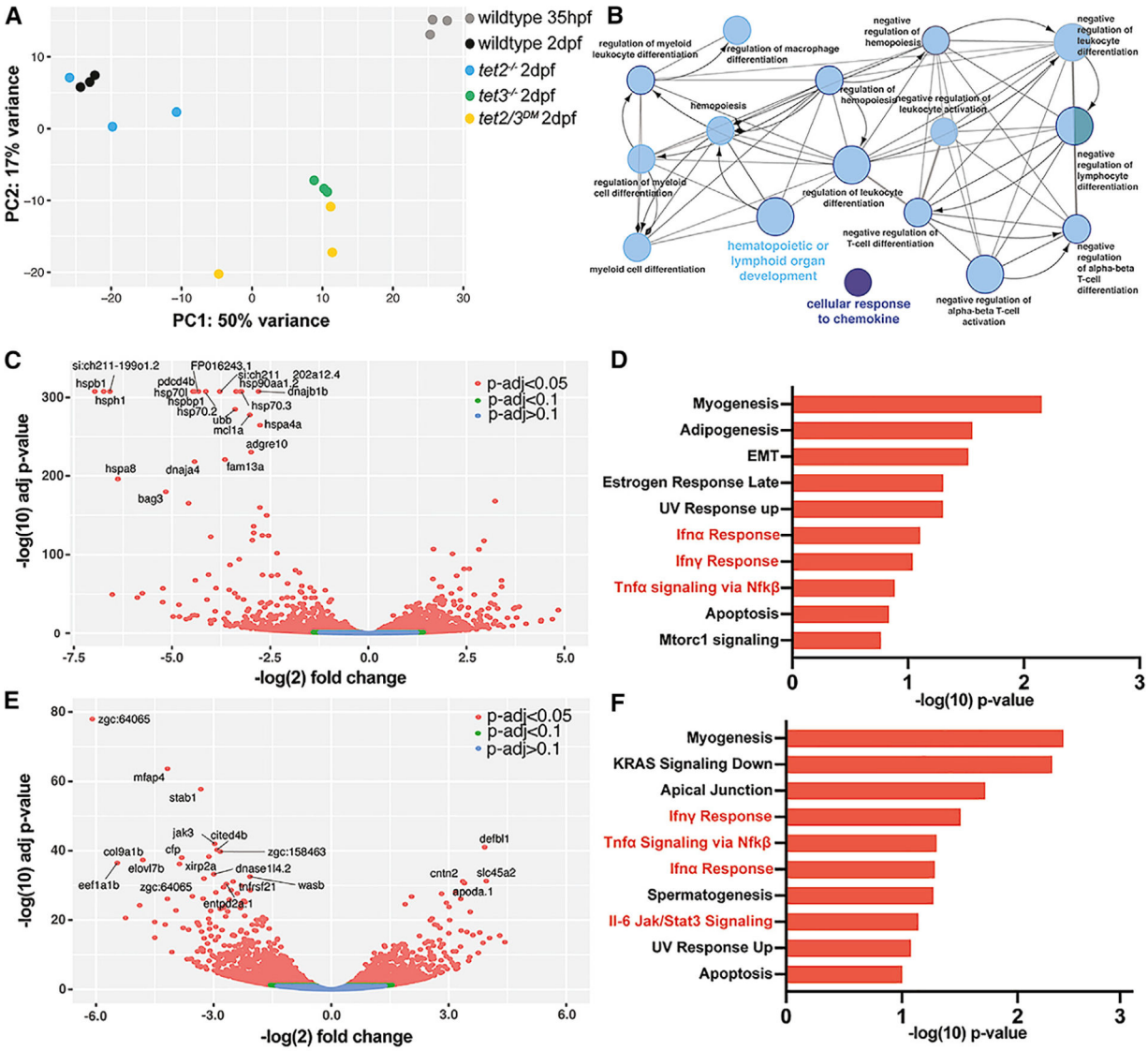

Figure 5. Transcriptional Profiling of *tet* Mutant Neutrophils Reveals Reduced Cytokine Response in *tet3*$^{-/-}$ and *tet2/3*^{DM}

Analysis of RNA sequencing from sorted neutrophils of 35-hpf wild-type, 2-dpf wild-type, 2-dpf *tet2*$^{-/-}$, 2-dpf *tet3*$^{-/-}$, and 2-dpf *tet2/3*^{DM} embryos.

(A) Principal component analysis for all samples, with three independent biological samples representing each genotype, as indicated by colored circles.

(B) Enriched GO terms related to hematopoiesis in genes downregulated in 2-dpf *tet2/3*^{DM} samples compared to 2-dpf wild-type samples.

(C) Volcano plot comparing 2-dpf *tet3*$^{-/-}$ and wild-type samples; the top 20 dysregulated genes are labeled.

(D) Top 10 hallmark GSEA terms downregulated comparing 2-dpf *tet3*$^{-/-}$ and wild-type samples; categories involved in cytokine response are highlighted in red.

(E) Volcano plot comparing 2-dpf *tet2/3*^{DM} and wild-type samples; the top 20 dysregulated genes are labeled.

(F) Top 10 hallmark GSEA terms downregulated comparing 2-dpf *tet2/3*^{DM} and wild-type samples; categories involved in cytokine response are highlighted in red. See also Figures S4 and S6 and Table S1.

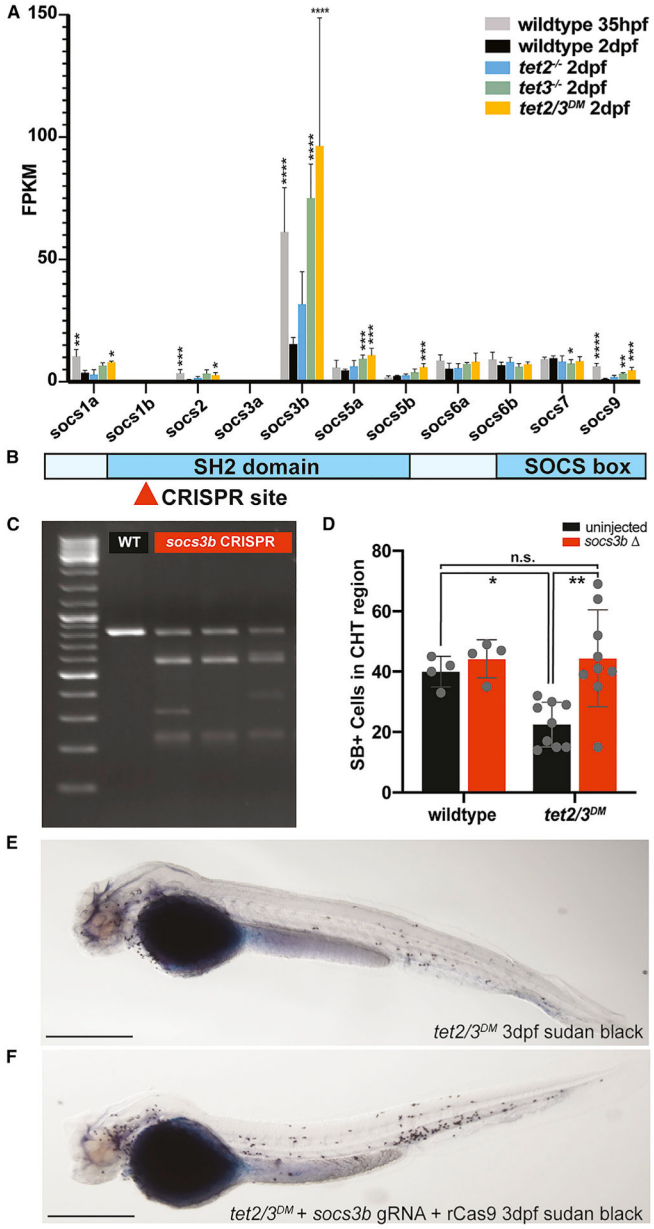

Figure 6. *Socs3b* mRNA Levels Are Increased in *tet* Mutant Neutrophils and Mutation of *socs3b* Rescues the Neutrophil Granulation Defect in *tet2/3*^{DM} Embryos

(A) Fragments per kilobase million (FPKM) for all SOCS family members across all genotypes; significance represents the adjusted p value from DESeq differential analysis comparing all other samples to wild type. *p-adj < 0.05, **p-adj < 0.01, ***p-adj < 0.001, ****p-adj < 0.0001.

(B) Schematic of *socs3b* gene structure and CRISPR target site.

(C) Representative T7 assay results demonstrating high gRNA targeting efficiency in 4 independent samples of F0 animals compared to wild-type uninjected embryos; 10 embryos per sample (WT).

(D) Quantification of SB+ cells in the CHT region of uninjected embryos (black bars) and F0 *socs3b* CRISPR injected embryos (red bars) at 3 dpf; n = 4–9/condition, *p < 0.05, **p < 0.01 by 2-way ANOVA with Tukey post hoc test.

(E and F) Representative images of SB staining in 2-dpf uninjected or *socs3b* mutated *tet2/3*^{DM} embryos. Scale bars represent 500 μm.

See also Figures S4 and S5.

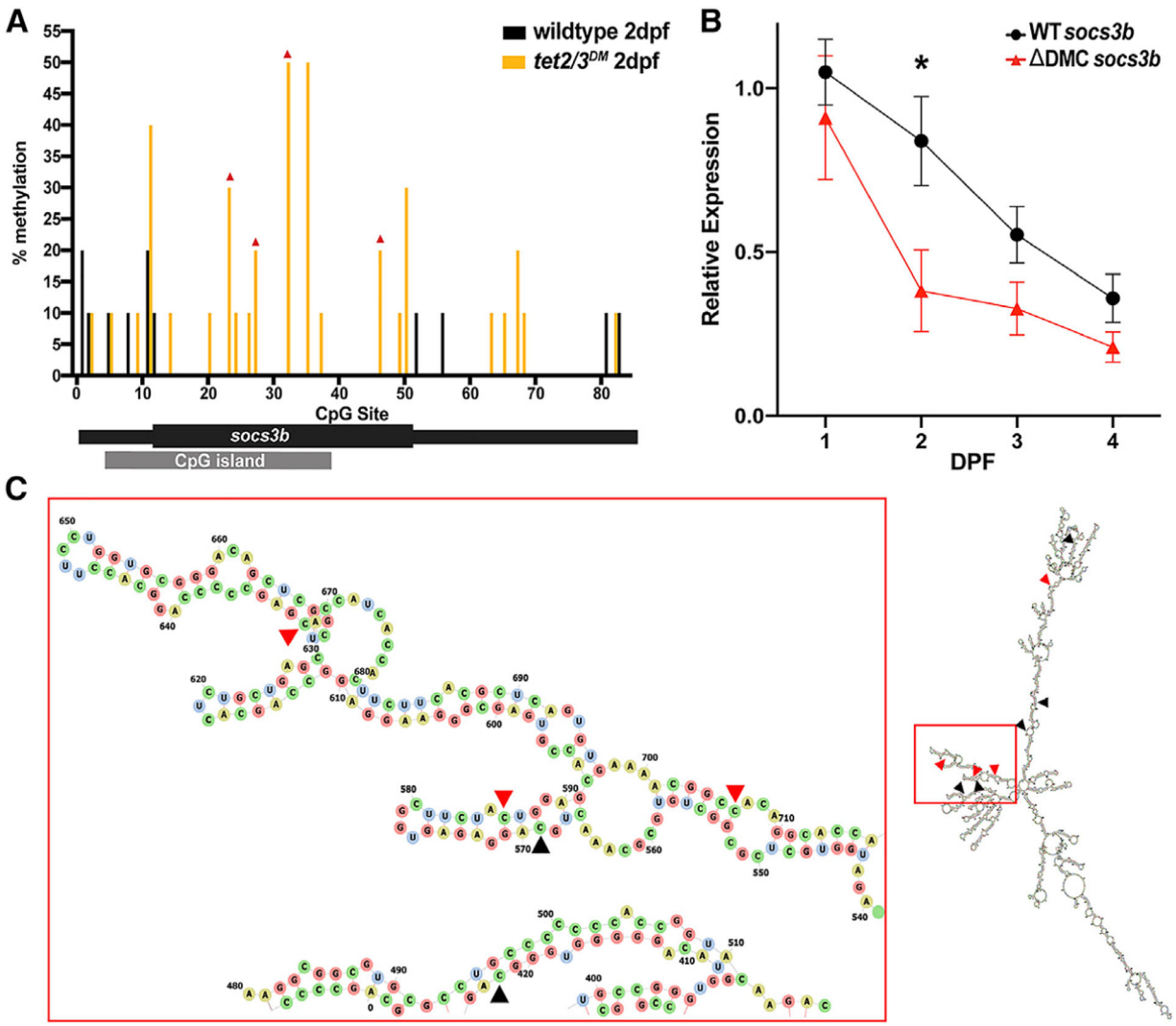

Figure 7. *Socs3b* mRNA Is Hypermethylated in *tet2/3*^{DM} Neutrophils

(A) RNA methylation status from RNA bisulfite-sequencing data for each CpG site in the *socs3b* locus for sorted wild-type or *tet2/3*^{DM} 2-dpf neutrophils; n = 10/condition. Red triangles indicate cytosines mutated in the differentially methylated cytosine (DMC) mutant mRNA used in the following experiment.

(B) Relative levels of *socs3b* mRNA at 1–4 dpf assessed by qRT-PCR that measures levels of the injected wild-type or DMC mutant transcripts; n = 6 groups of 5 embryos per data point, *p < 0.05 by 2-way ANOVA with Tukey post hoc test.

(C) Minimum free energy RNA structure of *socs3b*. DMCs are highlighted by triangles. Red triangles represent bases that were mutated in generating the DMC mutant *socs3b* mRNA and black triangles represent unedited bases. Inset: a close-up of an RNA arm with several DMCs closely packed together indicated by the red box in the full structure.

See also Figure S6 and Data S1.

KEY RESOURCES TABLE

REAGENT or RESOURCE	SOURCE	IDENTIFIER
Bacterial and Virus Strains		
One Shot TOP10 Chemically Competent *E. coli*	Invitrogen	Cat# C404006
Chemicals, Peptides, and Recombinant Proteins		
Sudan Black B	Sigma	Cat#199664
Critical Commercial Assays		
mMESSAGE mMACHINE	Invitrogen	AM1340
MEGAclear kit	QIAGEN	AM1908
RNeasy Mini kit	QIAGEN	74106
RNeasy Micro kit	QIAGEN	74004
Superscript VILO cDNA Synthesis Kit	Invitrogen	11754050
LightCycler 480 Sybr Green master mix	Roche	04–887-352–001
Ovation RNA-Seq System V2	Nugen	N/A
TruSeq RNA Library Prep Kit v2	Illumina	RS-122–2001
DNeasy Blood & Tissue Kits	QIAGEN	69506
EZ DNA Methylation-Direct kit	Zymo Research	D5021
EZ RNA Methylation Kit	Zymo Research	R5001
pHrodo phagocytosis assay	Invitrogen	A10026
Deposited Data		
Raw and analyzed data	This paper	GEO: GSE162435
Experimental Models: Organisms/Strains		
Zebrafish strain tet2$^{mk17/mk17}$, tet3$^{mk18/mk18}$ double-mutant (tet2/3^{DM}) Li et al., 2015	Li et al., 2015	
Zebrafish strain *mpx:GFP^{uwm1}*	Yoo and Huttenlocher, 2011	
Zebrafish strain *pu.1*:GFP^{zdf11}	Hsu et al., 2004	
Oligonucleotides		
socs3b CRISPR gRNA, see Table S2	This paper	
PCR primer sequences, see Table S2	This paper	
Recombinant DNA		
FH-TET3-pEF	Ko et al., 2010	ID:49446
FH-TET3-HxDmut-pEF	Ko et al., 2010	ID:127896
pCS2+*csf3b*	This paper	
pCS2+*socs3b*-wildtype	This paper	
pCS2+socs3b-CpG mutant	This paper	
Software and Algorithms		
FlowJo	Treestar	
ImageJ	Schneider et al., 2012	https://imagej.nih.gov/ij/
Bowtie2	Langmead and Salzberg, 2012	http://bowtie-bio.sourceforge.net/bowtie2/index.shtml
R	Cran	

REAGENT or RESOURCE	SOURCE	IDENTIFIER
Prism8	Graphpad	